

The proton whistler wave energization by finite frequency kinetic Alfvén wave: A numerical approach

Ravinder Goyal¹, R P Sharma², D N Gupta³ and Nidhi Gaur⁴

^{1,3}Department of Physics and Astrophysics, University of Delhi, INDIA.

(E-mail: ¹ravig.iitd@gmail.com, ³dngupta@physics.du.ac.in)

²Centre for Energy Studies, Indian Institute of Technology Delhi, INDIA.

(E-mail: rpsharma@ces.iitd.ac.in)

⁴School of Basic and Applied Sciences, KR Mangalam University, Gurgaon, INDIA

(E-mail: nidhiphysics@gmail.com)

ABSTRACT

The proton whistler waves have been detected in spacecraft measurements above the ionosphere of Earth. These are lightning impulses in dispersed form but are distinct from the more common whistlers both in tone and spectral characteristics. These are detected as propagating left-handed polarized waves. The present work focuses the mathematical formulation of transient behavior of proton whistler wave following its nonlinear interaction with small but finite amplitude kinetic Alfvén wave in solar wind plasma. The ponderomotive nonlinearity mediating the interaction phenomenon gets injected by pump (relatively higher frequency) kinetic Alfvén wave due to density variations which channelizes both waves. The numerical simulation technique employed for this nonlinear interaction study is done through solving second order differential equations governing the propagation of two waves and are coupled through density nonlinearity. The parameters used in this work belong to solar wind plasma at 1 AU. The respective magnetic and electric power spectra indicating turbulent transport of energies for kinetic Alfvén wave and proton whistler wave have been obtained and analyzed in the view of recent spacecraft observations of solar wind.

Keywords: kinetic Alfvén wave, ponderomotive nonlinearity, proton whistler wave, solar wind, turbulence.

I. INTRODUCTION

The turbulent nature of solar wind plasma is under debate and being studied extensively. The main point of now a days' concern is the dissipation range of solar wind turbulent spectrum at smaller MHD scales¹. At large scales, MHD approximations work efficiently².

Alfvénic MHD cascades^{3,4} are not found after spectral break when observed in higher time resolutions and proton cyclotron damping is supposed to suppress these cascades. In fact, the dispersive⁵ magnetosonic or whistler waves are dominant modes of that region of the power spectrum. Unlike Alfvén waves play a significant role in MHD turbulence⁶, the linear dispersion relation of whistler waves does not play vital role in spectral energy transfer even though these waves play significant role in EMHD turbulence. Kinetic Alfvén wave (KAW) and whistler carry energy cascades in the solar wind down to electron scales⁷. The significant role is played by whistlers in solar wind dissipation range with a relatively steeper spectrum⁸.

At cross-over frequency, the whistler waves flips its sense of polarization and gets converted into left-hand polarized proton whistler waves⁹. Proton whistlers are observed in the ionosphere¹⁰ as dispersed form of lightning impulses. These wave show a damping behavior at sub-proton gyrofrequencies. These waves have help researchers understand the dynamics of ionosphere and calculation of some vital parameters¹¹. Using Hall-MHD approach in their mathematical approach, Meyrand and Galtier¹² have studied the effect of left hand polarization on turbulent dynamics.

In the present work, we extend our previous analysis¹³ where we studied the steady state semi-analytical interaction of KAW with proton whistler wave in low frequency range. In the present work, we have used finite frequency regime for KAW to interact with low frequency

proton whistler in temporal domain and have used numerical simulation approach to study this nonlinear interaction.

In section 2, we give model equations of KAW in intermediate – β plasma and having x-z plane of propagation. Section 3 involves dynamics of weak proton whistler wave. The numerical approach is described in section 4 and section 5 contains discussion of outcomes. Summary and conclusions are given in section 6.

II. KINETIC ALFVEN WAVE (KAW) DYNAMICS

We consider the x-z plane propagation of KAW having finite amplitude and finite frequency with background magnetic field \tilde{B}_0 along z-axis in the magnetized plasma. The KAW is derived following the standard method followed by Goyal *et al.*¹³ in the form of a dynamical equation given as:

$$\frac{\partial^2 B_y}{\partial t^2} = -(V_{Te}^2 \lambda_e^2 + V_A^2 \rho_i^2) \frac{\partial^4 B_y}{\partial x^2 \partial z^2} + V_A^2 \left(1 - \frac{\delta n_s}{n_0}\right) \frac{\partial^2 B_y}{\partial z^2} + \frac{V_A^2}{\omega_{ci}^2} \left(1 - \frac{\delta n_s}{n_0}\right) \frac{\partial^4 B_y}{\partial t^2 \partial z^2} \quad (1)$$

Here, the background plasma density gets modified due to nonlinearity introduced by ponderomotive force of the KAW in intermediate- β plasma²⁷ and is given as follows:

$$\frac{\delta n_s}{n_0} = \phi(B_y B_y^*) \quad (2)$$

where $\phi(B_y B_y^*) = \exp(\gamma B_y B_y^*) - 1$, $\gamma = \left[(1 - \alpha_0 (1 + \delta)) / 16 \pi n_0 T \right] (V_A^2 k_{0z}^2 / \omega_0^2)$, $\alpha_0 = \omega_0^2 / \omega_{ci}^2$

$\delta = m_e k_{0x}^2 / m_i k_{0z}^2$ and k_{0x} (k_{0z}) is the wave vector perpendicular (parallel) to $\hat{z} B_0$.

Substituting the envelope solution $B_y = \tilde{B}(x, z, t) e^{i(k_{0x}x + k_{0z}z - \omega_0 t)}$ into Eq. (1), the nonlinear equation for KAW is written as:

$$\begin{aligned} & \frac{2i\omega_0(1+V_A^2k_{0z}^2/\omega_{ci}^2)}{V_A^2k_{0z}^2(1-\alpha_0)}\frac{\partial\tilde{B}}{\partial t} + \frac{2i}{k_{0z}(1-\alpha_0)}\left[\frac{k_{0z}^2(V_{Te}^2\lambda_e^2+V_A^2\rho_i^2)}{V_A^2}+(1-\alpha_0)\right]\frac{\partial\tilde{B}}{\partial z} + \frac{2ik_{0x}(V_{Te}^2\lambda_e^2+V_A^2\rho_i^2)}{V_A^2(1-\alpha_0)}\frac{\partial\tilde{B}}{\partial x} \\ & + \frac{1}{k_{0z}^2}\left[\frac{k_{0x}^2(V_{Te}^2\lambda_e^2+V_A^2\rho_i^2)}{V_A^2}+(1-\alpha_0)\right]\frac{\partial^2\tilde{B}}{\partial z^2} - \frac{(V_{Te}^2\lambda_e^2+V_A^2\rho_i^2)}{V_A^2(1-\alpha_0)}\frac{\partial^2\tilde{B}}{\partial x^2} - \phi(\tilde{B}\tilde{B}^*)\tilde{B} = 0 \end{aligned} \tag{3}$$

Equation (3) indicates the transient propagation of KAW which gets further modified to its final normalized (and hence dimensionless) form given by:

$$i\frac{\partial B}{\partial t} + i\xi_1\frac{\partial B}{\partial x} + \frac{\partial^2 B}{\partial x^2} + i\frac{\partial B}{\partial z} + \xi_2\frac{\partial^2 B}{\partial z^2} + (e^{|\beta|^2} - 1)B = 0 \tag{4}$$

with normalizing parameters given by $t_n = \frac{2\omega_0(1+V_A^2k_{0z}^2/\omega_{ci}^2)}{V_A^2k_{0z}^2(1-\alpha_0)}$; $x_n = \sqrt{(\rho_i^2 + \rho_s^2)/(1-\alpha_0)}$;

$$z_n = \frac{2}{k_{0z}(1-\alpha_0)}\left[\frac{k_{0x}^2(V_{Te}^2\lambda_e^2+V_A^2\rho_i^2)}{V_A^2}+(1-\alpha_0)\right]; \xi_1 = 2k_{0x}x_n \text{ and } \xi_2 = (1-\alpha_0)/2k_{0z}z_n.$$

III. DYNAMICS OF PROTON WHISTLER WAVE

The proton whistler wave is considered to be propagating along the z-direction i.e. along the background magnetic field lines. For the field variations given by $e^{i\omega t}$, the wave equation¹³ can be given as:

$$\frac{\partial^2 A_1}{\partial z^2} + \frac{1}{2}\left(1 + \frac{\epsilon_{+00}}{\epsilon_{zz}}\right)\frac{\partial^2 A_1}{\partial x^2} = \frac{1}{c^2}\frac{\partial^2}{\partial t^2}(\epsilon_+ A_1) \tag{5}$$

Here in the present study also, we are interested only in one mode and hence it is assumed that

$A_2 = 0$. Where

$$\epsilon_0 = 1 - \left(1 + \frac{\delta n_s}{n_0}\right)\left(\frac{\omega_p^2}{\omega^2}\right), \epsilon_{+0} = 1 - \left(1 + \frac{\delta n_s}{n_0}\right)\left[\frac{\omega_{pe}^2}{\omega(\omega + \omega_{ce})}\right] - \left(1 + \frac{\delta n_s}{n_0}\right)\left[\frac{\omega_{pi}^2}{\omega(\omega - \omega_{ci})}\right],$$

$$\epsilon_{-0} = 1 - \left(1 + \frac{\delta n_s}{n_0}\right)\left[\frac{\omega_{pe}^2}{\omega(\omega - \omega_{ce})}\right] - \left(1 + \frac{\delta n_s}{n_0}\right)\left[\frac{\omega_{pi}^2}{\omega(\omega + \omega_{ci})}\right].$$

ω_{pe} ($=\sqrt{4\pi n_0 e^2/m_e}$) is the electron plasma frequency and ω_{pi} ($=\sqrt{4\pi n_0 e^2/m_i}$) is the ion plasma frequency, ω_{ce} ($=eB_0/m_e c$) is the electron gyrofrequency, ω_{ci} ($=eB_0/m_i c$) being the ion gyrofrequency, ω is the frequency of proton whistler wave and we are considering low frequency proton whistler mode, $\omega/\omega_{ci} \approx 0.1$, $\delta n_s = n_e - n_0$ is the modification in density due to ponderomotive force of KAW, the pump wave.

We employ a plane wave solution in order to solve Eq. (5) which is given as:

$$A_1 = A(x, z, t) e^{i(k_+ z - \omega t)} \tag{6}$$

where $k_+ = \frac{\Omega}{c} \varepsilon_{+00}^{1/2}$, ε_{+00} being the linear part of ε_{+0} and A is the amplitude of complex nature.

Using above generalized plane wave solution in Eq. (5), Eq. (5) gets the form given by:

$$i \frac{\partial A}{\partial t} + \frac{ic}{\sqrt{\varepsilon_{+00}}} \frac{\partial A}{\partial z} + \frac{c^2}{2\omega \varepsilon_{+00}} \frac{\partial^2 A}{\partial z^2} + \frac{c^2}{4\omega \varepsilon_{+00}} \left(1 + \frac{\varepsilon_{+00}}{\varepsilon_{zz}}\right) \frac{\partial^2 A}{\partial x^2} - \frac{1}{2\varepsilon_{+00}} \left(-\frac{\omega_{pe}^2 (\delta n_s/n_0)}{(\omega + \omega_{ce})} - \frac{\omega_{pi}^2 (\delta n_s/n_0)}{(\omega - \omega_{ci})} \right) A = 0 \tag{7}$$

which can be rewritten into normalized and dimensionless form given by:

$$i \frac{\partial A}{\partial t} + ic_1 \frac{\partial A}{\partial z} + c_2 \frac{\partial^2 A}{\partial z^2} + c_3 \frac{\partial^2 A}{\partial x^2} + c_4 (e^{|\beta|^2} - 1) A = 0 \tag{8}$$

where $c_1 = \frac{c}{\sqrt{\varepsilon_{+00}}} \frac{t_n}{z_n}$; $c_2 = \frac{c^2}{2\omega \varepsilon_{+00}} \frac{t_n}{z_n^2}$; $c_3 = \frac{c^2}{4\omega \varepsilon_{+00}} \frac{t_n}{x_n^2}$; $c_4 = \frac{t_n}{2\varepsilon_{+00}} \left(-\frac{\omega_{pe}^2}{(\omega + \omega_{ce})} - \frac{\omega_{pi}^2}{(\omega - \omega_{ci})} \right)$

IV. NUMERICAL SIMULATIONS

A pseudo-spectral method is employed for present numerical analysis for space integration while for evolution in time we have adopted a predictor corrector scheme alongwith finite difference method having a step size $\Delta t = 10^{-4}$. The set of dynamical Eqs. (4) and (8) is then solved using the FORTRAN code fabricated keeping in view the propagation of two waves and their nonlinear interactions. The specifications of the code are: box having a size of $2\pi/a_x \times 2\pi/a_z$ with 64×64 grid points and the wave number of perturbation $a_x = a_z = 0.2$. A set of two

initial conditions is defined for solving these normalized partial differential equations. These initial conditions are: a hollow Gaussian variation in KAW magnetic field has been assumed while a Gaussian condition is considered for proton whistler which are defined as under:

$$B(x, z, 0) = a_0(x^2/r_1^2 + z^2/r_2^2) \exp(-x^2/r_1^2 - z^2/r_2^2) \quad (9)$$

$$B(x, z, 0) = a_1(1 + \varepsilon \exp(-x^2/r_1^2 - z^2/r_2^2)) \quad (10)$$

Where $a_0 = 0.2$ and $a_1 = 0.02$ respectively define the initial amplitudes of KAW and proton whistler waves, $r_1 = \alpha_x^{-1}$ and $r_2 = \alpha_z^{-1}$ and $\varepsilon = 0.01$ defines the perturbation magnitude.

$N = \sum_f |B_f|^2$ is defined as plasmon number for well-known nonlinear Schrödinger equation and conservation of plasmon number determines the accuracy of the code which is primarily retained before solving the set of dynamical equations. The computation was found to retain an accuracy of 10^{-5} associated with plasmon number. Apart from the normalizing parameters, the plasma parameters for solar wind used in present study are as follows: $\beta \approx 0.2$, are $B_0 \approx 6 \times 10^{-5} G$, $n_0 \approx 3 \text{ cm}^{-3}$, $T_e = 1.4 \times 10^5 K$, $T_i = 5.8 \times 10^5 K$. Using these values, the other parameters obtained: $V_A \approx 7.5 \times 10^6 \text{ cm/s}$, $V_{Te} \approx 1.4 \times 10^8 \text{ cm/s}$, $V_{Ti} \approx 6.923 \times 10^6 \text{ cm/s}$, $\omega_{ci} = 0.57 \text{ sec}^{-1}$, $\lambda_e = 3.07 \times 10^5 \text{ cm}$ and $\rho_i \approx 1.204 \times 10^7 \text{ cm}$, $\rho_s \approx 1.3 \times 10^7 \text{ cm}$. For $\omega_0/\omega_{ci} = 0.4$ and $k_{0x}\rho_s = 0.49$; $\omega_0 = 0.23 \text{ sec}^{-1}$, $k_{0x} \approx 3.6 \times 10^{-8} \text{ cm}^{-1}$ and $k_{0z} \approx 2.7 \times 10^{-8} \text{ cm}^{-1}$. For $\omega/\omega_{ci} = 0.1$; $\omega = 0.057 \text{ sec}^{-1}$.

V. RESULTS AND DISCUSSION

The intensity profile of normalized KAW magnetic field in the x-z plane is shown in Fig.1. The time advancement of the KAW intensity is clearly observed in the figures. The Fig. 1 illustrates that nonlinearity growth gives rise to localized structures having complex geography. The phenomenon of localization can be seen as: the pump KAW interacts nonlinearly with low frequency proton whistler wave by virtue of ponderomotive force giving rise to growth of

perturbation. The perturbation growth leads to formation of its own filaments which enforces pump KAW breakdown into localized structures. It can be further pointed out that as the time progresses, the KAW amplitudes firstly get increased and then decreases due to distribution of energy of KAW into subsequent structures thus forming small amplitude filaments. Dimensionality, Nonlinearity and initial conditions are some of the important factors affecting the localized structures of the KAW magnetic field. As evident from Fig. 1, the chosen initial conditions of simulation make their dominance on localization of KAW only at the commencing stage of evolution. But the effect of chosen initial conditions is no more dominant as the quasi steady state reaches and the system gets affected by other factors also and hence the localization phenomenon is achieved by the combined effects not solely because of chosen initial conditions.

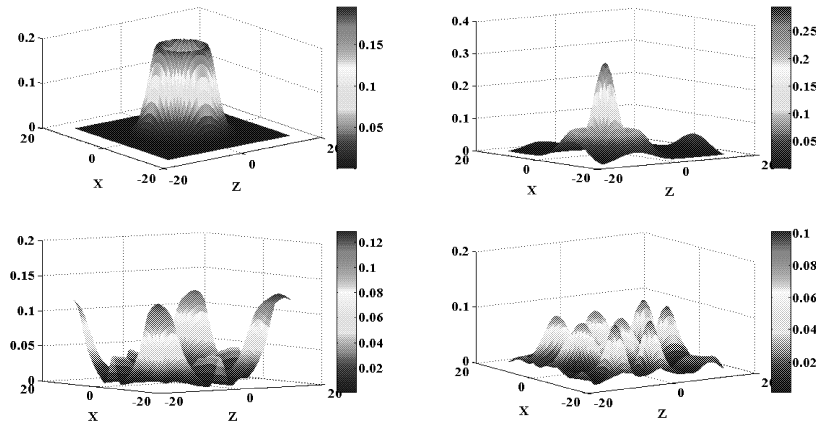


FIG.1 - The magnetic field intensity of KAW varying with x and z at $t = 0, 10, 25$ and 40 respectively.

The power spectra of KAW ($|B_f|^2$ varying with frequency f) and proton whistler ($|E_f|^2$ varying with frequency f) have also been studied in the present work which are shown in Figs. 2 and 3 respectively. The nonlinear coupling between KAW and relatively low frequency proton whistler leads to turbulence which is shown as the power spectra on frequency scales. These

spectra have been plotted at a fixed location (x, z) of the midpoint of longitudinal axis (z) and transverse axis (z). It is evident from the Figs. 2 and 3, the power spectra go steeper as one moves higher frequency scales. The solid line has been shown just for the sake of reference. This is not the actual scaling of the power spectrum. The observations by Saharoui *et al.*¹⁴ show the power spectrum having a scaling of $f^{2.5}$ as observed by FGM and STAFF-SC spacecrafts. Saharoui *et al.*¹⁴ depicted the dominance of KAW in sub-ion scales in solar wind based on their observed scalings. But in dissipation range, it could be the presence of KAW or whistler wave or both which lead to wave energy dissipation in other forms like heating and particle acceleration.

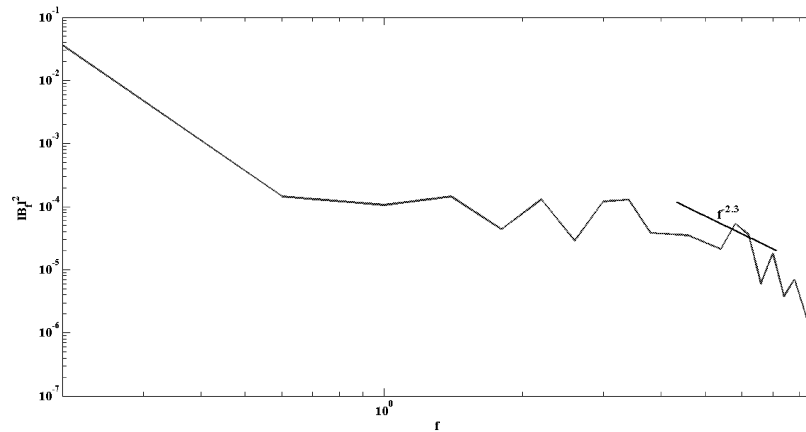


FIG.2 – Variation of normalized $|B_f|^2$ against f indicating KAW energy dissipation over a frequency range

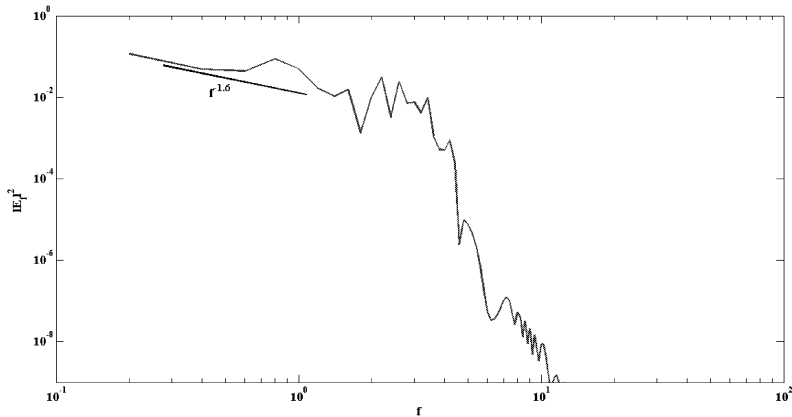


FIG.2 – Variation of normalized $|E_f|^2$ against f indicating proton whistler energy dissipation very quickly

VI. SUMMARY AND CONCLUSION

The present analysis is the extension of work which emphasized the interaction of KAW and proton whistler waves semi-analytically under paraxial approximation¹³. In the present study, the localization of large amplitude kinetic Alfvén waves at oblique incidence to the ambient magnetic field in intermediate- β plasmas applicable to solar wind has been investigated. The finite frequency KAW when propagates through plasma, due to ponderomotive force imposed by it creates density nonlinearity. The KAW gets self-focused due to this nonlinearity and filaments are formed. This channelization of KAW is attributed to the change in refractive index of the medium in which lens like structures are formed. The KAW when propagating through these structures gets focused and defocussed on regular intervals of time and space. Also, due to these nonlinear structures, KAW turbulence comes into picture which shows the energy impartation of KAW over a range of frequencies. The KAW turbulence observes a scaling of $f^{-2.3}$ which is very close to one observed by Saharoui *et al.*¹⁴ and hence suggests the dissipation

mechanism being mediated by KAWs. The density filaments created due to KAW energize weak proton whistler waves as well which also leads to turbulence. Although, proton whistler turbulence does not last over a large range of frequencies (energies) and dies down very quickly but still it follows Kolmogorov scaling ($f^{-1.6}$) in inertial range. At $\omega \approx \omega_{ci}$, there is resonant interaction between KAW and proton whistler wave. Due to which proton whistler may get maximum of energy of KAW and this energy may further be imparted to relatively high frequency whistler mode through mode coupling. These whistler waves as we know are very helpful in particle energization. In this paper, based upon the energy being carried by solar wind plasma into near earth environments, we can get the conclusion of particle energization/acceleration through wave-wave interactions which is currently under spotlight of all space and astrophysical research.

ACKNOWLEDGMENTS

This work is partially supported by SERB (India) under NPDF file number: PDF/2016/002568 and ISRO (India) under RESPOND program.

REFERENCES

- ¹D. Verscharen, E. Marsch, U. Motschmann and J. Müller, *Phys. Plasmas* **19**, 022305 (2012).
- ²F. Sahraoui, M. L. Goldstein, G. Belmont, P. Canu and L. Rezeau, *Phys. Rev. Lett.* **105**, 131101 (2010).
- ³R. J. Leamon, N. F. Ness, C. W. Smith and H. K. Wong, *AIP Conf. Proc.* **471**, 469 (1999).
- ⁴C. W. Smith, W. H. Matthaeus and N. F. Ness, *Proc. 21st Int. Conf. Cosmic Rays Graphics Services, Northfield* **5**, 280 (1990).
- ⁵O. Stawicki, S. P. Gary and H. Li, *J. Geophys. Res.* **106**, 8273 (2001).
- ⁶S. Galtier and A. Bhattacharjee, *Phys. Plasmas* **10**, 3065 (2003).
- ⁷F. Sahraoui, G. Belmont, M. L. Goldstein, *Astrophys. J.* **748**: 100 (2012).

- ⁸S. P. Gary, S. Saito and H. Li, *Geophys. Res. Lett.* **35**, L02104 (2008).
- ⁹A. K. Singh, Abhay K. Singh, D. K. Singh and R. P. Singh, *J. Atmos. Sol. Terr. Phys.* **60**, 551(1998).
- ¹⁰D. A. Gurnett, S. D. Shawhan, N. M. Brice and R. L. Smith, *J. Geophys. Res.* **70**, 7 (1965).
- ¹¹D. A. Gurnett and N. M. Brice, *J. Geophys. Res.* **71**, 15 (1966).
- ¹²R. Meyrand and S. Galtier, *Phys. Rev. Lett.* **109**, 194501 (2012).
- ¹³R. Goyal, R. P. Sharma, M. L. Goldstein and N. K. Dwivedi, *Phys. Plasmas* **20**, 122308 (2013).
- ¹⁴F. Sahraoui, M. L. Goldstein, P. Robert and Yu. V. Khotyaintsev, *Phys. Rev. Lett.* **102**, 231102 (2009).